COMMUNICATION

ChemComm
www.rsc.org/chemcomm

Fabrication and electrochemical properties of novel nanoporous platinum network electrodes†

Xinsheng Peng, Kallum Koczkur, Stephanie Nigro and Aicheng Chen*
Department of Chemistry, Lakehead University, Thunder Bay, Ontario, P7B 5E1, Canada.
E-mail: achen@lakeheadu.ca; Fax: 1-807-346-7775; Tel: 1-807-343-8318

Received (in Cambridge, UK) 9th August 2004, Accepted 17th September 2004
First published as an Advance Article on the web 25th October 2004

Three-dimensional nanoporous Pt networks with a high surface area were directly grown on titanium substrates through a simple hydrothermal-assisted seed growth method.

Recently, synthesis of nanostructured materials with high surface areas has received significant interest because the nanostructured materials may possess unique properties and a number of impressive applications in catalysis,[1] fuel cells[2] and chemical sensors.[3] Nanostructured Pt materials are very attractive due to their excellent electrocatalytic properties. A nanoporous Pt electrode is usually expected to exhibit much higher surface area than a smooth Pt electrode. The high surface area is vital to many electrochemical applications such as electrocatalysis and electrochemical sensors. Several methods have been developed for the preparation of nanostructured Pt. A mesoporous platinum film was prepared by electrodeposition of Pt into a liquid crystal surfactant template.[3,4a–c] With this method it is easy to control the size of the porous structures, but it is difficult and time-consuming to implement and to scale up the liquid crystal template techniques. Nanoporous Pt was recently produced by electrochemical dealloying, that is, selective dissolution of Cu or Zn from the CuPt or ZnPt binary alloys.[5a,b] This method is relatively easy; however, the preparation of the binary alloys requires special techniques, for instance, arc melting at high temperature, *e.g.*, 1000 °C[5a] or electrodeposition from a complex ionic liquid containing $ZnCl_2$.[5b] Titanium is widely used as a substrate because of its good corrosion-resistance and reasonable cost. Here, we report on a simple, templateless and surfactant-free, hydrothermal-assisted seed growth method for growing nanoporous platinum networks directly on Ti substrate to produce a novel electrode.

We fabricated a nanoporous Pt network electrode as follows: a Ti foil was washed with acetone followed by NANOpure water (18.2 MΩ cm), then etched in 30 wt% HCl at 80 °C for 10 min to remove the thin oxide layer on the titanium surface. Then Pt nanoparticles were electrodeposited on the etched Ti substrate at −20 mA cm^{-2} for 3 min from a solution composed of H_2PtCl_6 0.8 g l^{-1} and HCl 0.3 g l^{-1}. The treated Ti substrate was transferred into an autoclave containing ethylene glycol (EG), H_2PtCl_6 0.8 g l^{-1} and HCl 0.3 g l^{-1}, and heated at 100 °C for 10 h. After cooling to room temperature, the sample was washed again with acetone and Nanopure water, and the nanoporous Pt network electrodes were fabricated.

Scanning electron microscopy (SEM) was used to characterize the surface morphologies of the Ti substrates and nanoporous Pt networks. For comparison, an etched Ti substrate without Pt electrodeposition was also hydrothermal treated. Fig. 1(a) and (b) show the SEM images of the blank Ti substrate before and after the hydrothermal treatment, respectively. Pt particles and chain-like fibers are formed on the Ti surface. In contrast, Fig. 1(c) and (d) show the surface structure of the Ti substrate with Pt electrodeposition before and after the hydrothermal treatment.

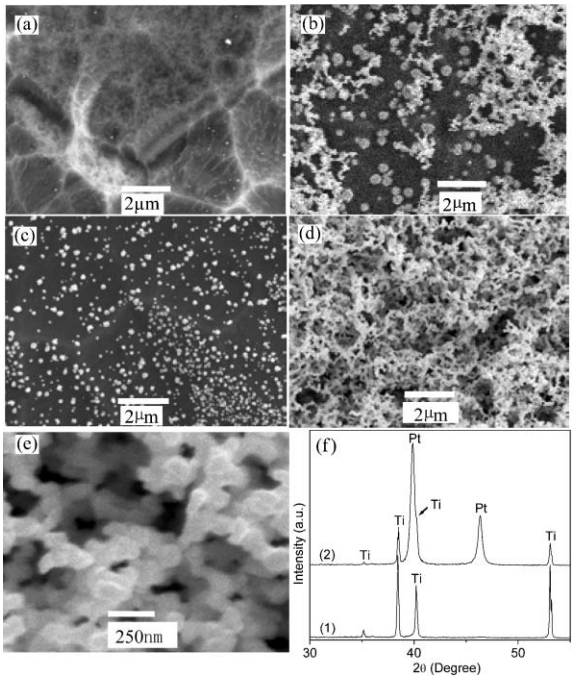

Fig. 1 SEM images: (a) a blank etched Ti substrate; (b) after the hydrothermal treatment of the blank Ti substrate; (c) an etched Ti substrate with electrodeposited Pt particles; (d), (e): after the hydrothermal treatment of the Ti substrate with electrodeposition of Pt; (f) XRD patterns, curves 1 and 2, recorded from (c) and (d).

Pt nanoparticles are dispersed on the Ti substrate through the electrochemical deposition. Surprisingly, nanoporous Pt networks were formed and completely covered on the substrate after the hydrothermal treatment; and the mass loading of the Pt is 0.16 mg cm^{-2}. Fig. 1(e) shows the Pt network, randomly porous with diameters of tens to hundreds of nanometers. Fig. 1(f) presents the XRD results of the sample with Pt electrodeposition before (curve 1) and after (curve 2) the hydrothermal treatment. The sharp Pt peaks observed in curve 2 further show the formation of large scale nanoporous platinum networks on the Ti substrate.

All the above results indicate that the electrodeposited Pt particles are favorable for the formation of nanoporous Pt networks. A seed growth mechanism has been reported for the formation of TiO_2 nanotube films,[6a] ZnO nanorod arrays,[6b] gold nanorods,[6c] and Te nanostructures:[6d] first homogenous nanoparticles are used as seeds transferred onto a solid substrate, then a sol–gel or colloid containing the same nanoparticles was used as the source material for the formation of the one-dimensional nanotubes or nanorods. Based on our SEM results, we propose that the nanoporous networks are formed by a seed growth process. At appropriate temperature and concentration of H_2PtCl_6, Pt nanoparticles are formed in the solution from the EG reduction of $PtCl_6^{2-}$. In this work the pre-electrodeposited Pt particles served as the seeds for the growth of the hydrothermally formed Pt nanoparticles to form the nanoporous network shown in Fig. 1(d).

† Electronic supplementary information (ESI) available: Equivalent circuit used to fit the impedance spectra presented in Fig. 2(d). Table S1: The values for the parameters R_{ct}, CPE_T, CPE_P and their associated error % computed by fitting of the experimental EIS data (Fig. 2(d)). See http://www.rsc.org/suppdata/cc/b4/b412677g/

DOI: 10.1039/b412677g

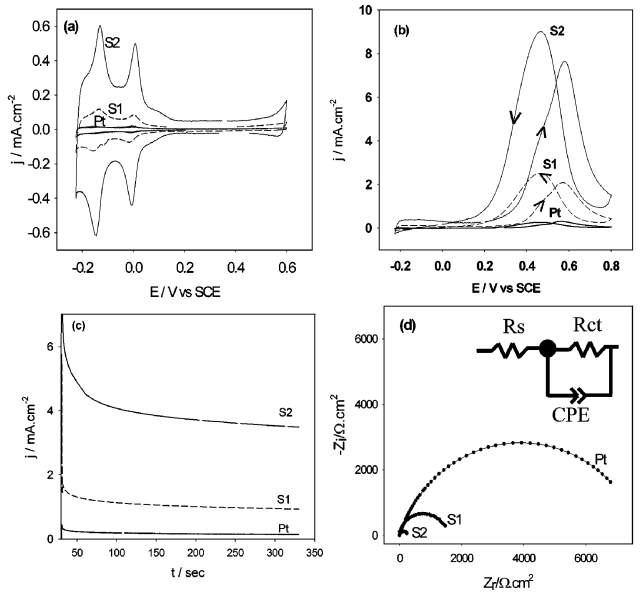

Fig. 2 Cyclic voltammograms of polycrystalline Pt, S1 and S2 (a) in 0.5 M H_2SO_4 solution and (b) in 0.5 M H_2SO_4 + 0.1 M CH_3OH at a potential scan rate of 20 mV s^{-1}; (c) Chronoamperometry at 600 mV and (d) Electrochemical impedance spectra (EIS) at 300 mV of the polycrystalline Pt, S1 and S2 in 0.5 M H_2SO_4 + 0.1 M CH_3OH. The inset in Fig. 2(d) is the equivalent circuit model for fitting the EIS data.

Electrochemical techniques, as described in our previous study,[7a] were used to characterize the electrochemical properties of the nanoporous Pt network electrodes. Hydrogen adsorption and desorption is a powerful technique to determine the active surface area of a Pt electrode.[7b] Fig. 2(a) shows three cyclic voltammogrametric (CV) curves for a polycrystal Pt electrode, the blank Ti substrate after hydrothermal treatment (S1), and the Ti substrate with Pt electrodeposition after the hydrothermal treatment (S2) in a 0.5 M H_2SO_4 solution at a potential sweep rate of 20 mV s^{-1}. All the samples have consistent hydrogen adsorption/desorption behavior: two reversible peaks at approximately −0.16 and −0.019 V. The integrated intensity of the peaks represents the number of Pt sites available for hydrogen adsorption/desorption, *i.e.* actual surface area. In calculating the hydrogen adsorption charge on electrode surfaces, we assume that double layer charging current is constant over the whole potential range. The hydrogen adsorption charge (Q_H) of S1 is 0.83 mC cm^{-2}, which is approximately four times larger than that of the smooth polycrystalline Pt (0.21 mC cm^{-2}). The Q_H of S2 is 4.13 mC cm^{-2}, which indicates that the actual surface area of the nanoporous platinum electrodes is 20 times larger than that of the polycrystalline Pt electrode.

One important factor in direct methanol fuel cell is the activity of the catalyst towards methanol oxidation.[1,8a–c] Fig. 2(b) shows three CV curves recorded in a 0.1 M CH_3OH + 0.5 M H_2SO_4 solution at 20 mV s^{-1}. Both S1 and S2 show higher current densities, broader peaks, and a lower onset of methanol electro-oxidation than the polycrystalline Pt electrode. The methanol oxidation peak on the nanoporous Pt network electrode S2 is over 20 times larger than that on the polycrystalline platinum. The onset potential for methanol electrooxidation is at 0.4 V for the Pt electrode, but at 0.3 V for S1, and even much lower for S2 (0.15 V). Chronoamperometry was employed to further test the activity of these three electrodes: the electrode potential was held at 0.0 V for 30 s, and then stepped up to 0.6 V and held there for 300 s. Fig. 2(c) shows the three current–time curves. Steady-state currents of methanol electrooxidation on the three electrodes are achieved after 300 s. At t = 300 seconds, the steady-state currents for the polycrystalline Pt, S1 and S2 are 0.14, 0.93 and 3.50 mA cm^{-2}, respectively. The steady-state current for the nanoporous Pt network electrode is 25 times larger than that for the polycrystalline Pt electrode. These results are very consistent with the CV studies shown in Fig. 2(a) and (b).

Electrochemical impedance spectroscopy was used to determine the charge transfer resistance and the capacitance of these three electrodes during methanol electrooxidation. Fig. 2(d) presents three Nyquist plots recorded in a 0.1 M CH_3OH + 0.5 M H_2SO_4 solution at an electrode potential of 300 mV, where Z_i and Z_r are the imaginary and real components of the impedance. The frequency was changed from 40 kHz to 25 mHz. It can be seen that the impedance on both the imaginary and real axes of S1 and S2 are significantly lower than those of Pt wire. An equivalent electric circuit, as shown in the inset of Fig. 2(d), was used to fit the experimental data (denoted by symbols) and the fitted results are represented by lines (Fig. 2(d)). In the $R_s(R_{ct}CPE)$ circuit, R_s represents the uncompensated solution resistance, while the parallel combination of the charge transfer resistance (R_{ct}) and the constant phase element (CPE) takes into account the methanol adsorption and oxidation. The parallel combination ($R_{ct}CPE$) leads to a depressed semi-circle in the corresponding Nyquist impedance plot. The CPE is defined by two components, CPE_T and CPE_P. If CPE_P equals 1, then the CPE is considered a capacitor C_{dl}. As shown in Fig. 2(d), the proposed model can fit the EIS data effectively. All electrodes showed a CPE_P result of approximately 0.9 which means the CPE_T values are close to the C_{dl}. The CPE_T value for S2 is much larger than that of the polycrystalline Pt. In contrast, the charge transfer resistance for the polycrystalline Pt electrode is 7178 Ω, which is over 25 times larger than that for the nanoporous Pt network electrode S2 (275 Ω). All the above results show that the activity of the nanoporous Pt network electrode is significantly enhanced compared to the polycrystalline Pt electrode.

In conclusion, three-dimensional nanoporous Pt network electrodes have been successfully fabricated by a simple, hydrothermal-assisted seed growth process. Electrochemical studies show that the actual surface area of the nanoporous Pt network electrode is over 20 times larger than that of a polycrystalline Pt electrode and that the nanoporous Pt network electrode has a much higher current during electrochemical oxidation of methanol. The nanoporous Pt network electrodes possess a large surface area and high electrocatalytic activity, which is especially desirable for electrochemical sensor design and catalyst development for fuel cells and electrochemical treatment of wastewater.

The work was supported by a grant from the Natural Sciences and Engineering Research Council of Canada (NSERC).

Notes and references

1 Z. H. Zhou, S. L. Wang, W. J. Zhou, G. X. Wang, L. H. Jiang, W. Z. Li, S. Q. Song, J. G. Liu, G. Q. Sun and Q. Xin, *Chem. Commun.*, 2003, 394.
2 K. Y. Chan, J. Ding, J. W. Ren, S. A. Cheng and K. Y. Tsang, *J. Mater. Chem.*, 2004, **14**, 505.
3 S. Park, T. D. Chung and H. C. Park, *Anal. Chem.*, 2003, **75**, 3046.
4 (*a*) H. Boo, S. Park, B. Ku, Y. Kim, J. H. Park, H. C. Kim and T. D. Chung, *J. Am. Chem. Soc.*, 2004, **126**, 4524; (*b*) S. A. G. Evans, J. M. Elliott, L. M. Andrews, P. N. Bartlett, P. J. Doyle and G. Denuault, *Anal. Chem.*, 2002, **74**, 1322; (*c*) J. M. Elliott, G. S. Attard, P. N. Bartlett, N. R. B. Coleman, D. A. S. Merckel and J. R. Owen, *Chem. Mater.*, 1999, **11**, 3602.
5 (*a*) D. V. Pugh, A. Dursun and S. G. Corcoran, *J. Mater. Res.*, 2003, **18**, 216; (*b*) J. F. Huang and I. W. Sun, *Chem. Mater.*, 2004, **16**, 1829.
6 (*a*) Z. R. R. Tian, J. A. Voigt, J. Liu, B. Mckenzie and H. F. Xu, *J. Am. Chem. Soc.*, 2003, **125**, 12384; (*b*) X. J. Feng, L. Feng, M. H. Jin, J. Zhai, L. Jiang and D. B. Zhu, *J. Am. Chem. Soc.*, 2004, **126**, 62; (*c*) J. D. Zhang, M. Kambayashi and M. Oyama, *Electrochem. Commun.*, 2004, **6**, 683; (*d*) U. K. Gautama and C. N. R. Rao, *J. Mater. Chem.*, 2004, **14**, 2530.
7 (*a*) A. Chen and B. Miller, *J. Phys. Chem. B*, 2004, **108**, 2245; (*b*) D. Kardash and C. Korzeniewski, *Langmuir*, 2000, **16**, 8419.
8 (*a*) S. Park, Y. Xie and M. J. Weaver, *Langmuir*, 2002, **18**, 5792; (*b*) Z. L. Liu, X. Y. Ling, X. D. Su and J. Y. Lee, *J. Phys. Chem. B*, 2004, **108**, 8234; (*c*) W. Z. Li, C. H. Liang, W. J. Zhou, J. S. Qiu and Z. H. Zhou, *J. Phys. Chem. B*, 2003, **107**, 6292.